Building and Test a Controller of the Robotic Cane for Walking Assistance

Phi Van Lam[*a)] Non-member, Yasutaka Fujimoto[*b)] Senior Member

In this paper, a robotic cane is proposed with a totally completed hardware to support people who need physical assistance to stand or walk. The robotic cane can stand with the only omni-directional wheel based on the principle of inverted pendulum. It can return the balancing point in a short time when it is influenced by an external force. A controller of the robotic cane is also designed, and its operation is verified with the good experiment results.

Keywords: Inverted pendulum, robotic cane, walking assistance, omni-directional wheel, assistant device.

1. Introduction

When life standards become higher and higher, the rate of aging population increases dramatically, specially, in developed countries like Japan. This leads to a fact that the elderly may need to be supported by the younger people in daily life. But, it is not easy for the young to help the elderly in modern life. To solve this problem, there have been many studies to manufacture devices and robots instead of people to do this work. Injured, elderly and disabled people may have difficulties in standing or walking without physical assistance. In many cases, these people totally rely on assistant devices such as single-legged canes [1]-[2], four-legged canes, fall prevention [3], and wheel chairs [4]-[5]. However, users always wish that they could stand or walk independently all only minimally rely on assistant devices. Accordingly, there is an urgent requirement for research of new alternative devices with much more active assistance to support people to walk or stand. In this research, we propose a simplified-structure, no need to wear as a wearable robot [6] and light-weight of the robotic cane to realize a simple and light-weight robot which is not inferior to the above mentioned assistant devices. The concept of the robotic cane was mentioned in [2]. However, there has not been any completed hardware of the robotic cane which is proposed in this paper. Besides, its controller is designed with a good performance.

2. Hardware of the robotic cane

A robotic cane in Fig. 1 (a) which includes a grip handle (1), a rod (2), a center controller, a balance control sensor and batteries inside the box (3), brushless motors (4), and a gearbox (5) including a motorized omni-directional wheel with minor wheels.

The balancing control sensor provides a balancing signal corresponding to an orientation of the robotic cane. The center controller receives the balance signal from the balance control sensor and calculates a balancing velocity of the motorized omni-directional wheel based at least in part on the balance signal and an inverted pendulum control algorithm. The center controller may further provide a drive signal to the motorized omni-directional wheel in accordance with the calculated balancing velocity. The calculated balancing velocity

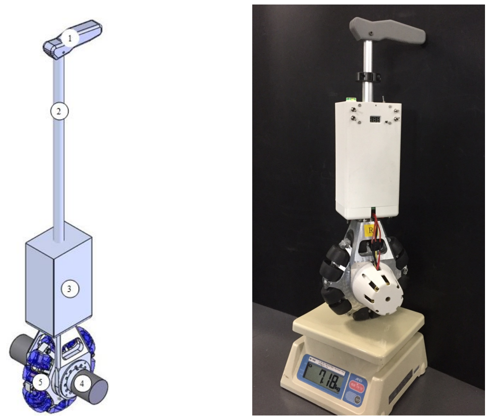

(a) Solidworks (b) Hardware

Fig. 1. The robotic cane for walking assistance

is a speed and direction of the motorized omni-directional wheel to retain the robotic cane in a substantially upright position. Depending on the control signal from the algorithm in the controller, the robotic cane can stand or move.

The robotic cane can move in different directions by using only two motors combined with omni-directional wheel design. The basic operating principle of the robotic cane with four basic possibilities of motion. The cane moves forwards or backwards when two motors rotate clockwise or counterclockwise. Otherwise, it moves on the right or left when two motors rotate in two different directions.

By using gyroscope sensor, we can detect the angles the rod of the robotic cane when it moves or stands. Through velocity of the robotic cane, we determine the user's force which is necessary to control the robotic cane. Moreover, two motor drivers are applied to the robotic cane to help it to run and control the current output to brushless motors easily

a) Correspondence to: phi-lam-pv@ynu.jp
b) Correspondence to: fujimoto@ynu.ac.jp
* Fujimoto Laboratory, Department of Electrical and Computer Engineering, Yokohama National University, Yokohama, Japan 240-8501.

Table 1. Explanation of symbols

Symbol	Explanation
T_1	Rotational kinematics of Wheel
T_2	Rotational kinematics of cane
T_3	Translational kinematics of the wheel
T_4	Translational kinematics of the cane
T	Kinematics total
V [kg·m^3/s]	Potential total
J_ϕ [kg·m^2]	Inertia of the cane
J_θ [kg·m^2]	Inertia of the wheel
D_ϕ [N.m.s/rad]	Viscous friction coefficient of cane
D_θ [N.m.s/rad]	Viscous friction coefficient of wheel
l [m]	Length of the cane
l_c [m]	Center of mass of the cane
m [kg]	Mass of cane
M [kg]	Mass of wheel
τ [N.m]	Actuation torque
g [m^2/s]	Gravitational acceleration
r [m]	Radius of the wheel

and perfectly when received control signals from the center controller depend on the algorithm designed. The hardware of the robotic cane is shown in Fig. 1 (b) with about 7.2 kg including batteries.

3. Mathematical model of the robotic cane

The relationship between the rotation angle of the omni-directional wheel and the rotation angle of two motors is expressed in the equation (1) and (2). The major wheel angle, the minor wheel angle, the angle of left-side motor and right-side motor are expressed as θ_{Pitch}, θ_{Roll}, θ_R and θ_L, respectively.

$$\theta_{Pitch} = G\frac{\theta_R + \theta_L}{4} \quad (1)$$

$$\theta_{Roll} = G\frac{\theta_R - \theta_L}{2} \quad (2)$$

where G is a ratio of the gearbox, it is designed as $G = 1/25$.

The standard coordinate system in Fig. 2 has two basic planes: the sagittal plane - xz, and lateral plane - yz. For sagittal plane, the robotic cane can be regarded as an inverted pendulum with a large wheel. Similarly, it can be considered an inverted pendulum with small wheels in the lateral plane. The torque of the left motor and the right one is calculated by the equations (1) and (2). Motion equations of the robotic cane are obtained from Lagranges equations (3). Equations of motion in the sagittal plane and the lateral plane are the same except for their input parameters.

$$\begin{cases} \frac{\mathrm{d}}{\mathrm{dt}}\left(\frac{\partial \mathrm{L}}{\partial \dot{\theta}}\right) - \frac{\partial \mathrm{L}}{\partial \theta} + \frac{\partial \mathrm{F}_{fr}}{\partial \dot{\theta}} = \tau \\ \frac{\mathrm{d}}{\mathrm{dt}}\left(\frac{\partial \mathrm{L}}{\partial \dot{\phi}}\right) - \frac{\partial \mathrm{L}}{\partial \phi} + \frac{\partial \mathrm{F}_{fr}}{\partial \dot{\phi}} = 0 \end{cases} \quad (3)$$

where, L is the Lagrangian:

$$L = T - V \quad (4)$$

$$\mathrm{F}_{fr} = \frac{1}{2}\mathrm{D}_\phi \dot{\phi}^2 + \frac{1}{2}\mathrm{D}_\theta \dot{\theta}^2 \quad (5)$$

$$V = \mathrm{mglcos}\phi \quad (6)$$

$$\begin{cases} \mathrm{T}_1 = \frac{1}{2}\mathrm{J}_\theta(\dot{\theta} - \dot{\phi})^2 \\ \mathrm{T}_2 = \frac{1}{2}\mathrm{J}_\phi \dot{\phi}^2 \\ \mathrm{T}_3 = \frac{1}{2}\mathrm{Mr}^2(\dot{\theta} - \dot{\phi})^2 \\ \mathrm{T}_4 = \frac{1}{2}\mathrm{m}\left\{ \left[\frac{\mathrm{d}}{\mathrm{dt}}(\mathrm{r}(\theta - \phi) - \mathrm{lsin}\phi)\right]^2 + \left[\frac{\mathrm{d}}{\mathrm{dt}}(\mathrm{lcos}\phi)\right]^2 \right\} \end{cases} \quad (7)$$

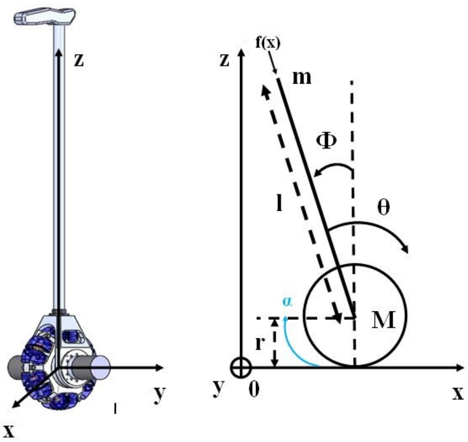

Fig. 2. Coordinate system of the robotic cane

$$T = \sum_{i=1}^{4} T_i \quad (8)$$

Parameters are denoted in Table 1. Replacing the formulas (4), (5), (6), (7) in the equation (3) and these equations are nonlinear, we have the following equation:

$$\begin{bmatrix} \mathrm{H}_{11} & \mathrm{H}_{12} \\ \mathrm{H}_{21} & \mathrm{H}_{22} \end{bmatrix} \begin{bmatrix} \ddot{\phi} \\ \ddot{\theta} \end{bmatrix} + \begin{bmatrix} \mathrm{b}_1 \\ \mathrm{b}_2 \end{bmatrix} = \begin{bmatrix} 0 \\ \tau \end{bmatrix} \quad (9)$$

where, H_{ij} is an element of the inertia matrix, b_i is a nonlinear term expressed as follows:

$$\mathrm{H}_{11} = \mathrm{J}_\theta + (\mathrm{M} + \mathrm{m})\,\mathrm{r}^2 + 2\mathrm{mrlcos}\phi + \mathrm{J}_\phi + \mathrm{ml}^2 \quad (10)$$

$$\mathrm{H}_{12} = \mathrm{H}_{21} = -\mathrm{J}_\theta - (\mathrm{M} + \mathrm{m})\,\mathrm{r}^2 - \mathrm{mrlcos}\phi \quad (11)$$

$$\mathrm{H}_{22} = \mathrm{J}_\theta + (\mathrm{M} + \mathrm{m})\,\mathrm{r}^2 \quad (12)$$

$$\mathrm{b}_1 = -\dot{\phi}^2\mathrm{mrlsin}\phi - \mathrm{mglsin}\phi + \mathrm{D}_\phi\dot{\phi} \quad (13)$$

$$\mathrm{b}_2 = \dot{\phi}^2\mathrm{mrlsin}\phi + \mathrm{D}_\theta\dot{\theta} \quad (14)$$

From the equations (9)-(14), it is seen that the system of the robotic cane is a nonlinear system, and the nonlinear controller is based on approximate feedback linearization is applied to control this system [7]. Let u be a new input. Then, the actuation torque τ is obtained as follows:

$$\tau = (H_{22} - \frac{H_{12}H_{21}}{H_{11}})u - \frac{H_{21}b_1}{H_{11}} + b_2 \quad (15)$$

Nonlinear system as the equation bellow:

$$\begin{cases} \dot{x} = f(x) + g(x)u \\ y = h(x) \end{cases} \quad (16)$$

Lie Algebra method is expressed as follows:

$$L_f h(x) = \sum_{i=1}^{n} \frac{\partial h(x)}{\partial x} f_i(x) = \frac{\partial h(x)}{\partial x} f(x) \quad (17)$$

with the input signal u is:

$$u = \frac{v - L_f{}^r h(x)}{L_g L_f{}^{r-1} h(x)} \quad (18)$$

where $v = y^{(r)}$ and:

$$v = -\sum_{i=0}^{r-1} \lambda_i (y^{(i)} - y_{ref}^{(i)}) \cdots\cdots (19)$$

We define y as a function of ϕ and θ as:

$$y = \sigma_1(\phi) + \sigma_2(\theta) \cdots\cdots (20)$$

Expanding the derivation of y by t:

$$\dot{y} = \frac{\partial \sigma_1(\phi)}{\partial \phi}\dot{\phi} + \frac{\partial \sigma_2(\theta)}{\partial \theta}\dot{\theta} \cdots\cdots (21)$$

$$\ddot{y} = \left\{ \begin{array}{l} \frac{\partial^2 \sigma_1(\phi)}{\partial \phi^2}\dot{\phi}^2 + \frac{\partial^2 \sigma_2(\theta)}{\partial \theta^2}\dot{\theta}^2 - \frac{b1}{H_{11}}\frac{\partial \sigma_2(\theta)}{\partial \theta} \\ +(\frac{H_{12}}{H11}\frac{\partial \sigma_1(\phi)}{\partial \phi} - \frac{\partial \sigma_2(\theta)}{\partial \theta})u \end{array} \right\} \cdots\cdots (22)$$

To use a linear controller, we need to cancel high levels:

$$\frac{H_{12}}{H11}\frac{\partial \sigma_1(\phi)}{\partial \phi} - \frac{\partial \sigma_2(\theta)}{\partial \theta} = 0 \cdots\cdots (23)$$

By using this way, we have a new variable y and its derivatives as follow:

$$y = \int_0^{\phi} \frac{H_{11}}{H_{12}} d\phi + \theta \cdots\cdots (24)$$

$$\dot{y} = \frac{H_{11}}{H_{12}}\dot{\phi} + \dot{\theta} \cdots\cdots (25)$$

$$\ddot{y} = \frac{\partial}{\partial \phi}\frac{H_{11}}{H_{12}}\dot{\phi}^2 - \frac{b_1}{H_{12}} \cdots\cdots (26)$$

$$y^{(3)} \simeq \frac{\partial^2}{\partial \phi^2}\frac{H_{11}}{H_{12}}\dot{\phi}^3 - \frac{\partial}{\partial \phi}\frac{b_1}{H_{12}}\dot{\phi} - 2(\frac{\partial}{\partial \phi}\frac{H_{11}}{H_{12}})\frac{b_1}{H_{11}}\dot{\phi} \cdot (27)$$

comparing with the equation (18), and we have $r = 4$ and:

$$u = \frac{v - L_f{}^4 h(x)}{L_g L_f{}^3 h(x)} \cdots\cdots (28)$$

$$v = -\sum_{i=0}^{3} \lambda_i (y^{(i)} - y_{ref}^{(i)}) \cdots\cdots (29)$$

From the equation (27), we calculate derivative $y^{(3)}$ by t one more time, and receive two parts of input signal in the equation (28) as $L_f{}^4 h(x)$ and $L_g L_f{}^3 h(x)$.

With disturbances from the sensor or external forces and the equation (3) is changed to the equation:

$$\left\{ \begin{array}{l} \frac{d}{dt}\left(\frac{\partial L}{\partial \dot{\phi}}\right) - \frac{\partial L}{\partial \phi} + \frac{\partial F_{fr}}{\partial \dot{\phi}} = 0 - d_1 \\ \frac{d}{dt}\left(\frac{\partial L}{\partial \dot{\theta}}\right) - \frac{\partial L}{\partial \theta} + \frac{\partial F_{fr}}{\partial \dot{\theta}} = \tau - d_2 \end{array} \right. \cdots\cdots (30)$$

But it is difficult for us to control the inverted pendulum to stand without being kept by user, and in [7], the author showed that we can use a disturbance observer to estimate them and control the system to be more stable:

$$\begin{array}{l} \dot{\xi} = -K\xi + K^2 \frac{\partial L}{\partial \dot{q}} + K(\frac{\partial L}{\partial q} - \tau_{all}) \\ \hat{d} = \xi + K\frac{\partial L}{\partial q} \end{array} \cdots\cdots (31)$$

$$\begin{bmatrix} d_1 \\ d_2 \end{bmatrix} = \begin{bmatrix} -l\cos\phi - r & -l\sin\phi \\ r & 0 \end{bmatrix} \begin{bmatrix} fx \\ fz \end{bmatrix} \cdots\cdots (32)$$

To make the robotic cane balanced, a gravity system is necessary:

Table 2. Measured parameters of the robotic cane

Symbol	Sagittal plane	Lateral plane
T_s [s]	1e-4	1e-4
D_ϕ [N.m.s/rad]	0.025	0.03
D_θ [N.m.s/rad]	0.025	0.03
l [m]	0.37	0.445
m [kg]	4.66	7.0
M [kg]	2.60	0.26
g [m^2/s]	9.80621	9.80621
r [m]	0.1	0.025

$$\begin{bmatrix} -lmg\sin\phi_{ref} \\ 0 \end{bmatrix} = \begin{bmatrix} 0 \\ \tau \end{bmatrix} - \begin{bmatrix} -l\cos\phi_{ref} - r & -l\sin\phi_{ref} \\ r & 0 \end{bmatrix} \begin{bmatrix} fx \\ fz \end{bmatrix} \quad (33)$$

compare between two equations (32) and (33) we have:

$$\phi_{ref} = \sin^{-1}\left(\frac{\hat{d}_1}{mgl}\right) \cdots\cdots (34)$$

$$\theta_{ref} = \theta \cdots\cdots (35)$$

4. Experiments in the designed hardware of the robotic cane

With the experiment on the designed hardware of the robotic cane, we measure parameters of the system and show them on Table 2. With the parameters here, we have three tests with it: first is test the work of the robotic cane in normal case; second is stability mode as a standing alone of the robotic cane; and the last of test is moving with user together and support to user standing when they tend to fall down.

Firstly, we test the control algorithm which controls the robotic cane to stand without being kept by user, the result is shown in Fig. 3. The position of the robotic cane in Fig. 3 (a)-(b) and in Fig. 5 indicates that its position hardly move.

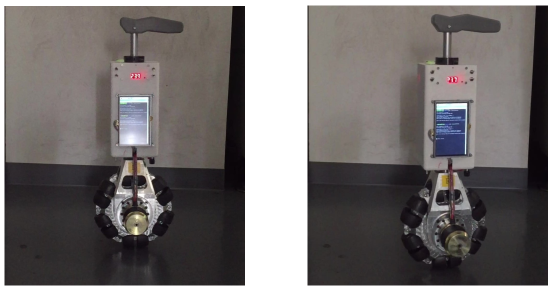

(a) At the 50th second (b) After 40th second

Fig. 3. Stability around balancing point

Secondly, we test the case in which the user needs the robotic cane to support to stand or move. The result which is cut from a video is shown in Fig. 6. The status of the rod always tends to go to the zero degree like the case when the robotic cane stands alone.

When following user and support them to moving together in Fig. 6 (a); next step when user tends to fall backward in Fig. 6 (b) the robotic cane will run too fast to the standing state as go backward for change the position of rod for help user go back the equilibrium position as the same with other state in Fig. 6 (c) the robotic cane can support big force

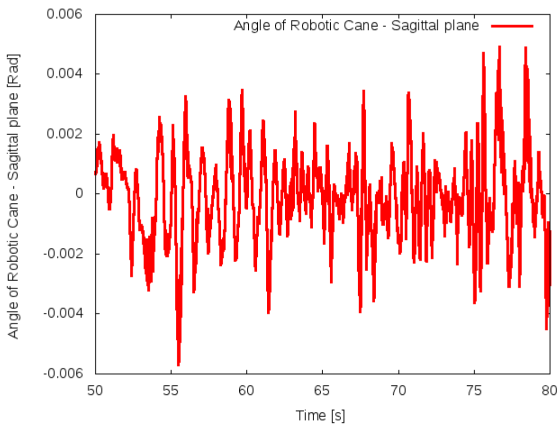

Fig. 4. Angle of the robotic cane while stability

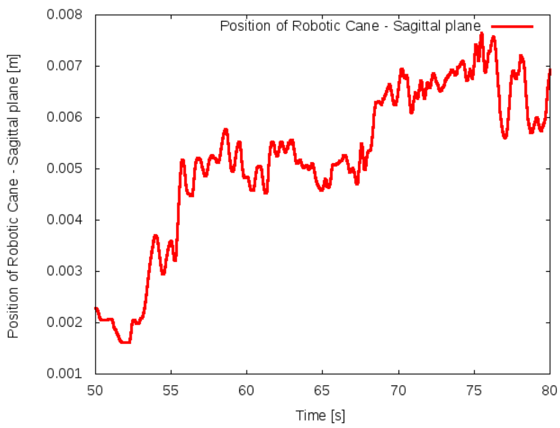

Fig. 5. Position of the robotic cane while stability

(a) Stand (b) Fall backward (c) Fall forward

Fig. 6. The robotic cane support user walking

through the handle to user for help people easy to standing or moving everywhere.

In Fig. 7 and Fig. 8, the result shows data in three cases in Fig. 6. The period from second 10^{th} to second 30^{th}, the robotic cane moved with the user, it stood up straight. In the next status, the user tended to fall backwards, the robotic cane immediately moved forwards with the speed like the speed of the user (in Fig. 8 from second 30^{th} to second 35^{th}) to help the user to go back the balance status. In this case, we can see that the different to angle signal is quite small and changed very slowly in Fig. 7.

Therefore, the position of the robotic cane also responded the signal similarity. In the last case, when the user tended to fall forwards with a quite big speed in Fig. 7 from second 35^{th} to second 40^{th}, the robotic cane responded corresponding to the requirement time to response. A sudden increase could be seen in Fig. 8 at the same time, but after a very short

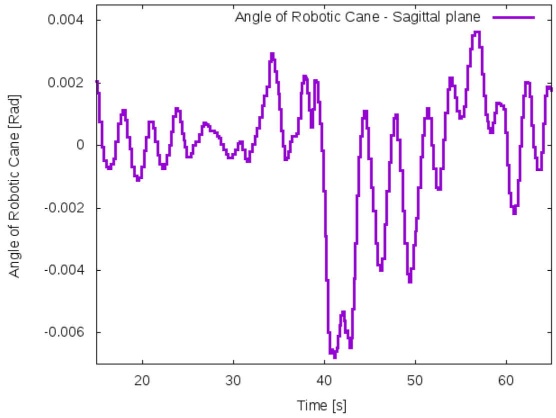

Fig. 7. Angle of the robotic cane while support user

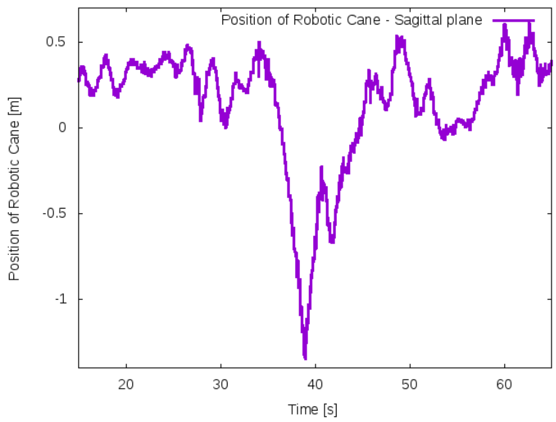

Fig. 8. Position of the robotic cane while support user

time in Fig. 8, it could go back the balance position.

5. Conclusions

The authors designed the hardware of the robotic cane using omni-directional wheel and high processing controller for walking assistance and designed controller using linearization of nonlinear control and for control the robotic cane moving, standing alone, support user move or stand as a normal people.

References

(1) K. Shimizu, et al., *"A Robotic Cane for Walking Support Using Two Control Modes"*, SAMCON2016, (2016).

(2) Y. Ota, et al., *"Robotic cane devices"*, US Patent Application, pub. no. US2013/0041507A1, (2013).

(3) S. Nakagawa, et al., *"Tandem Stance Avoidance Using Adaptive and Asymmetric Admittance Control for Fall Prevention"*, IEEE Transactions on Neural Systems and Rehabilitation Engineering, (2015).

(4) C. Zhu, et al., *"A new type of omnidirectional wheelchair robot for walking support and power assistance"*, Ph. D. thesis, proc. IEEE/RSJ IROS, pp. 6028-6033, (2010).

(5) T. Kagawa, et al., *"Admittance based control of wheelchair typed omnidirectional robot for walking support and power assistance"*, RO-MAN, 2010 IEEE, (2010).

(6) T. Kagawa, et al., *"Optimization-Based Motion Planning in Joint Space for Walking Assistance With Wearable Robot"*, IEEE transactions on robotics, pp. 415-424, (2015).

(7) I. A. Smad, et al., *"Nonlinear control of mechanical systems with application to monowheel robot"*, Ph. D. thesis, Yokohama National University, (2009).